

Locking of length scales in two-band superconductors

M. Ichioka

*Department of Physics, RIIS, Okayama University, Okayama 700-8530, Japan**

V. G. Kogan

Ames Laboratory, US Department of Energy, Ames, Iowa 50011, USA

J. Schmalian

*Institut für Theorie der Kondensierten Materie und Institut für Festkörperphysik,
Karlsruher Institut für Technologie, D-76131 Karlsruhe, Germany*

(Dated: February 8, 2022)

A model of a clean two-band s-wave superconductor with cylindrical Fermi surfaces, different Fermi velocities $v_{1,2}$, and a general 2×2 coupling matrix $V_{\alpha\beta}$ is used to study the order parameter distribution in vortex lattices. The Eilenberger weak coupling formalism is used to calculate numerically the spatial distributions of the pairing amplitudes Δ_1 and Δ_2 of the two bands for vortices parallel to the Fermi cylinders. For generic values of the interband coupling V_{12} , it is shown that, independently of the couplings $V_{\alpha\beta}$, of the ratio v_1/v_2 , of the temperature, and the applied field, the length scales of spatial variation of Δ_1 and of Δ_2 are the same within the accuracy of our calculations. The only exception from this single length-scale behavior is found for $V_{12} \rightarrow 0$, i.e., for nearly decoupled bands.

PACS numbers: 74.20.-z, 74.25.Uv

I. INTRODUCTION

Just at the dawn of the theory of multiband superconductors, it was established that near the critical temperature T_c , the coherence lengths, which set the length scales of spatial variation of the pairing amplitudes of the bands, are in fact the same, notwithstanding differences in zero- T BCS lengths $\xi_{0,\alpha} \propto v_\alpha/T_c$ (α is the band index and v_α is the Fermi velocity) [1]. This result has been “rediscovered” in the recent debate on the proper form of Ginzburg-Landau (GL) theory of two-band superconductors [2, 3]. This debate was triggered by extensive studies of multiband MgB_2 which prompted the formulation of two order-parameter GL energy functionals to allow for different length scales $\xi_1 \neq \xi_2$ associated with the two underlying bands, see [4, 5] and references therein. One of the predictions of these models was an intervortex attraction at distances large with respect to the London penetration depth. The observation of vortex clustering in MgB_2 in very small fields was considered as evidence for asymptotic intervortex attraction [6].

While it is established [1–3] that near T_c , where the GL-expansion is justified, any generic superconductor with finite interband coupling is governed by a single superconducting order parameter with one coherence length, it was pointed out in Ref. [3] that this does not have to be true away from T_c . Novel behavior is expected especially in cases with different Fermi velocities of the bands and for very weak interband coupling; this requires to turn to microscopic descriptions of superconductors

that are applicable at all temperatures. Interesting calculations of this kind were performed in Refs. [7, 8] and showed that away from T_c and for a very weak inter-band coupling the length scales ξ_1 and ξ_2 are indeed not equal, in particular for low temperatures and at small magnetic fields.

However, there are several reasons why in real materials the inter-band coupling is not as weak as was assumed in Refs. [7, 8]. First, the ever present Coulomb repulsion will inevitably give rise to off-diagonal matrix elements in band-representation, even though the usual renormalization of the Coulomb pseudopotential tends to reduce interband interactions more strongly than intraband interactions [9]. For MgB_2 the latter effect was analyzed and is rather moderate [9]: the bare interband Coulomb interaction is about half of the bare intraband interaction; renormalizations only reduce this ratio by another factor of 2, yielding interband Coulomb interactions that are approximately 25% of the intraband couplings. Second, the matrix elements of the electron-lattice coupling within and between electronic bands are for the important optical phonon branches a priori of the same order of magnitude. Even for MgB_2 , where the observation of a Leggett-mode in the Raman spectrum [10] is evidence for comparatively weak interband coupling, a careful analysis of the inter- and intraband interactions reveals that the former is still about 20% of the larger and similar to the smaller of the intraband interactions [9, 11–14]. In other systems, such as the recently discussed iron-based superconductors is even argued that the interband coupling is the dominant source of pairing, see e.g. Refs. [15, 16].

Further support for comparatively large interband coupling comes from an analysis of recent Scanning Tunnel-

* ichioka@okayama-u.ac.jp

ing Microscopy (STM) measurements of the density of states (DOS) distribution within the vortex lattice at low temperatures in several two-band compounds [17, 18]. For a single-band material one can construct a phenomenological model to relate the measured zero-bias DOS distribution $N(\mathbf{r})$ to the pairing amplitudes $|\Delta(\mathbf{r})|$ in the lattice unit cell [17]. This procedure is readily extended to a two-band situation, for which $N(\mathbf{r})$ depends on both ξ_1 and ξ_2 . The fit to the STM data for NbSe₂ and for NbSe_{1.8}S_{0.2} showed that $\xi_1 \approx \xi_2$ at $T = 0.15 \text{ K} \ll T_c$. The same procedure has been applied to the novel superconductor CaKFe₄As₄ with $T_c \approx 35 \text{ K}$ and the zero-field tunneling spectrum having clearly two-gap features, again with the result $\xi_1 \approx \xi_2$ at sub-Kelvin temperatures and at all fields examined [18].

These theoretical considerations and observations motivated us to re-examine the question of the relative values of ξ_1 and ξ_2 in two-band superconductors within a microscopic approach that covers a broad temperature and magnetic field regime. In particular, the analysis of the STM-data suggests that the emergence of one common length-scale is a much more robust phenomenon than one would expect for moderately coupled multi-band system. Thus, we aim at clarifying the issue of when the coupling between two superconducting bands becomes sufficiently strong to give rise to a common length scale and under what conditions two separate length scales of the band-order parameters emerge.

To this end, we use a “brute-force” numerical procedure of solving Eilenberger equations for a vortex lattice in the two-band case developed in studies of MgB₂ [19]. We consider a weak-coupling model of a two-band superconductor with two Fermi surface parts having different Fermi velocities and study the spatial variation of the pairing amplitudes $\Delta_{1,2}(\mathbf{r})$ of the two bands within the vortex lattice unit cell. While we analyze this model over a wide range of parameters, we do not focus on a specific application for a particular material. Rather, we intend to clarify general properties of the spatial dependency of $\Delta_{1,2}(\mathbf{r})$. Substantially different values of the Fermi velocities notwithstanding, the coherence lengths proportional to the vortex core size defined as $\xi_{1,2}^{(c)} \propto (d|\Delta_{1,2}|/dr)_{r \rightarrow 0}^{-1}$ (r is the distance from the vortex center) turn out nearly the same for all choices of coupling constants $V_{\alpha\beta}$ examined ($\alpha, \beta = 1, 2$) except the case of nearly decoupled condensates $V_{12}/V_{11} \leq 0.1$.

In the limit $V_{12} \ll V_{11}$ our results agree with previous calculations [7, 8]. However, as soon as $V_{12}/V_{11} \geq 0.1$, we obtain $\xi_1 = \xi_2$, insensitive to details of coupling $V_{\alpha\beta}$, temperature, and field. Given the exponential dependence of the superconducting gap on the coupling constants, comparatively weakly coupled systems with $V_{12}/V_{11} \geq 0.2 \cdots 0.5$ may easily display interesting multi-band behavior, such as collective fluctuations of the relative phase of the bands [10]. However, our results show that the system is nevertheless governed by a single order-parameter characterized by a single length scale.

II. APPROACH

We consider two-band system with two cylindrical Fermi surfaces ($\alpha = 1, 2$) both oriented parallel to the same crystal axis (the c -axis) and with Fermi velocities $\mathbf{v}_\alpha(\mathbf{k}) = v_\alpha(\cos \phi, \sin \phi)$. \mathbf{k} is the Fermi momentum and ϕ the corresponding azimuth. The magnetic field is applied along \mathbf{c} as well, i.e. the field is parallel to the axis of the cylinder. For simplicity, the bands normal densities of states are assumed the same: $N_{0,1} = N_{0,2} = N_0$ (the total DOS per spin $N(0) = 2N_0$). This assumption will not affect any of our results qualitatively and can easily be dropped. It still allows for distinct values of the Fermi velocities of the bands. We set $v_2 = 3v_1$ to assure substantially different coherence lengths in the limit of fully decoupled bands. The 2×2 coupling matrix $V_{\alpha\beta}$ is assumed symmetric: $V_{12} = V_{21}$.

Our approach is based on the quasiclassical version of the weak-coupling BCS theory for anisotropic Fermi surfaces and order parameters [20]. This theory is formulated in terms of Eilenberger functions f , f^+ and g (Gor’kov’s Green’s functions averaged over the energy):

$$(2\omega + \mathbf{v}_\alpha \cdot \mathbf{\Pi})f_\alpha = 2\Delta_\alpha g_\alpha, \quad (1)$$

$$g_\alpha^2 = 1 - f_\alpha f_\alpha^+, \quad \alpha = 1, 2. \quad (2)$$

Here $\mathbf{\Pi} = \mathbf{\nabla} + 2\pi i \mathbf{A}/\phi_0$ with vector potential \mathbf{A} and flux quantum ϕ_0 . $\omega = \pi T(2n + 1)$ are fermionic Matsubara frequencies with integer n ; hereafter ω and T are measured in energy units, i.e. $\hbar = k_B = 1$. The equation for f^+ is obtained from Eq. (1) by taking the complex conjugate and replacing $\mathbf{v} \rightarrow -\mathbf{v}$.

The pairing amplitudes satisfy the self-consistency relations:

$$\Delta_\alpha(\mathbf{r}) = 4\pi T N_0 \sum_{\beta, \omega} V_{\alpha\beta} \langle f(\omega, \mathbf{k}, \mathbf{r}) \rangle_\beta, \quad (3)$$

where the sum over positive Matsubara frequencies is extended up to ω_D , the analog of Debye frequency for electro-phonon mechanism; $\langle f(\omega, \mathbf{k}, \mathbf{r}) \rangle_\beta$ stands for the average over the Fermi cylinder of the band β . The contribution of the α -band to the current density is

$$\mathbf{J}_\alpha(\mathbf{r}) = -4\pi |e| N_0 T \text{Im} \sum_{\omega > 0} \langle \mathbf{v} g(\omega, \mathbf{k}, \mathbf{r}) \rangle_\alpha, \quad (4)$$

and the total current density is

$$\mathbf{J} = \mathbf{J}_1 + \mathbf{J}_2 = \mathbf{\nabla} \times (\mathbf{\nabla} \times \mathbf{A}) c / 4\pi. \quad (5)$$

The vector potential is taken in the form $\mathbf{A}(\mathbf{r}) = (\mathbf{B} \times \mathbf{r})/2 + \tilde{\mathbf{A}}(\mathbf{r})$, where the magnetic induction $\mathbf{B} = (0, 0, B)$ is the field averaged over the vortex lattice cell and $\tilde{\mathbf{A}}(\mathbf{r})$ represents the variable part of the field which is periodic in the vortex lattice and has zero spatial average. The unit vectors of the triangular vortex lattice are chosen as $\mathbf{u}_1 = (a_0, 0, 0)$ and $\mathbf{u}_2 = (\frac{1}{2}a_0, \sqrt{3}a_0/2, 0)$, where the intervortex spacing is $a_0 = (2\phi_0/\sqrt{3}B)^{1/2}$. We use periodic boundary conditions for the unit cell of the vortex

lattice and take into account the order parameter phase winding around each vortex [21].

Throughout the paper, we use Eilenberger units for the first band if it would have been single ($V_{12} = V_{22} = 0$): $R_1 = \hbar v_1 / 2\pi T_{c1}$ is taken as a unit length ($R_1 \approx 0.88 \xi_{01}$ where ξ_{01} is the zero- T BCS coherence length of the “bare” first band). Fermi velocities are normalized to v_1 , the magnetic field is measured in units of $B_1 = \phi_0 / 2\pi R_1^2$ and the current density in $cB_1 / 4\pi R_1$, the energy unit is πT_{c1} , and T_{c1} is the transition temperature in the single-band limit. In these units, Eqs. (1) and (4) take the form:

$$(\omega + \mathbf{v}_\alpha \cdot \nabla) f_\alpha = \Delta_\alpha g_\alpha - i \mathbf{v}_\alpha \cdot [(\mathbf{B} \times \mathbf{r})/2 + \tilde{\mathbf{A}}] f_\alpha, \quad (6)$$

$$\mathbf{J}_\alpha(\mathbf{r}) = -\frac{2T}{\kappa_1^2} \sum_{\omega > 0} \langle \mathbf{v} \text{Im } g(\omega, \mathbf{k}, \mathbf{r}) \rangle_\alpha. \quad (7)$$

Hereafter we keep the same notation for dimensionless quantities as for their dimensional counterparts; we will indicate explicitly if common units are needed.

The quantity $\kappa_1 = \phi_0 T_{c1} / \pi \hbar^2 v_1^2 \sqrt{2N_0}$ has the same order of magnitude as the GL parameter for one-band isotropic case, $\kappa_{GL} = 3\phi_0 T_c / \hbar^2 v^2 \sqrt{7\zeta(3)N(0)}$. However, κ_1 does not have the meaning of the penetration-depth-to-coherence-length ratio for the two-band system[2, 3], rather it is a convenient dimensionless material parameter.

The dimensionless self-consistency equations take the form:

$$\Delta_\alpha(\mathbf{r}) = 2tN_0V_{11} \sum_{\beta, \omega} \frac{V_{\alpha\beta}}{V_{11}} \langle f(\omega, \mathbf{k}, \mathbf{r}) \rangle_\beta, \quad (8)$$

$$\pi e^{-\gamma} T_{c1} = 2\omega_D \exp(-1/N_0 V_{11}), \quad t = T/T_{c1} \quad (9)$$

where γ is the Euler constant. In our calculations we set the cutoff frequency $\omega_D = 40 T_{c1}$ and $\kappa_1 = 4$. The numerical procedure is outlined in the Appendix.

The profiles of the pairing amplitudes $|\Delta_\alpha(\mathbf{r})|$ in real space are fitted by a 5th-order polynomial near the vortex center along the nearest neighbor vortex direction. We estimate the vortex core size $\xi_\alpha^{(c)}$ from

$$\Delta_\alpha(\mathbf{r}) = \Delta_{m,\alpha} \frac{r}{\xi_\alpha^{(c)}} + O(r^2), \quad j = 1, 2 \quad (10)$$

near the vortex center. $\Delta_{m,\alpha}$ is the maximum value of $|\Delta_\alpha(\mathbf{r})|$ within the unit cell.

III. V_{12} OF THE SAME ORDER AS V_{11}

First, we present our results for $V_{12} = 0.32V_{11}$. In order to see the effect of the coupling in the second band, we consider two cases: $V_{22} = 0$ and $V_{22} = 0.32V_{11}$.

The profiles of $|\Delta_1(\mathbf{r})|$ and $|\Delta_2(\mathbf{r})|$ are shown in Fig. 1(a). Near the vortex center, both $|\Delta_1(\mathbf{r})|$ and $|\Delta_2(\mathbf{r})|$ recover over the same lengths; this is seen most directly in panel (b) where nearly constant ratios $|\Delta_2(\mathbf{r})|/|\Delta_1(\mathbf{r})|$ are shown. In the presence of finite intraband coupling of the second band V_{22} , the amplitude of the pair potential of this band increases, with

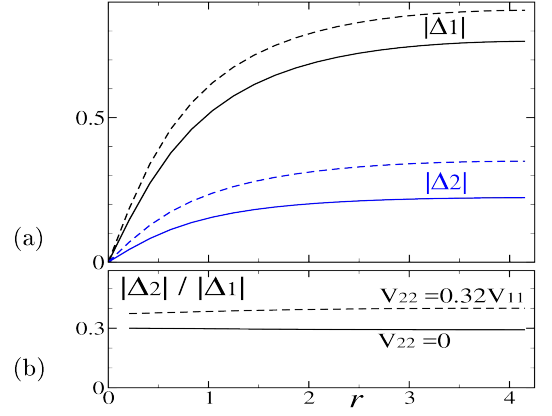


FIG. 1. (Color online) (a) Pairing amplitudes $|\Delta_1(\mathbf{r})|$ and $|\Delta_2(\mathbf{r})|$ (in units πT_{c1}) vs distance r (in units of $R_1 = \hbar v_1 / 2\pi T_{c1}$) from the vortex center to the midpoint between nearest neighbor vortices. In this calculation, $V_{12}/V_{11} = 0.32$, $t = T/T_{c1} = 0.5$, and $B = 0.1$ (in units $\phi_0 / 2\pi R_1^2$). Solid lines are for $V_{22} = 0$, dashed lines are for $V_{22}/V_{11} = 0.32$. (b) Nearly constant ratios $|\Delta_2(\mathbf{r})|/|\Delta_1(\mathbf{r})|$ imply the same length scales for both pairing amplitudes.

$|\Delta_2(\mathbf{r})|/|\Delta_1(\mathbf{r})| \sim 0.4$, as expected. The spatial dependence of the two pair potentials is however the same.

Temperature dependences of the core radii $\xi_\alpha^{(c)}$ and of the maximum value $\Delta_{m,\alpha}$ are given in Fig. 2. While $\Delta_{m,\alpha}$ are slightly smaller than those in zero field (dotted line) as they should, the T -dependence of $\Delta_{m,\alpha}$ is similar to that at zero field. Nearly constant ratios $\Delta_{m,2}/\Delta_{m,1}$ are ≈ 0.3 for $V_{22} = 0$ and ≈ 0.4 for $V_{22} = 0.34V_{11}$. As the temperature increases, this ratio changes little: from 0.291 to 0.295 for $V_{22} = 0$, and from 0.406 to 0.392 for $V_{22} = 0.32V_{11}$, respectively. Within our analysis we also reproduce Kramer-Pesch shrinking of the vortex core sizes $\xi^{(c)}$ on cooling [22–24], see Fig. 2(c,d). Thus, we obtain $\xi_2^{(c)} \approx \xi_1^{(c)}$ in the whole temperature range. While it is expected [1–3] that $\xi_2^{(c)}/\xi_1^{(c)} \rightarrow 1$ for $T \rightarrow T_c$, our finding of numerically very similar length scales over a broad temperature regime is rather surprising.

The field dependencies of the pairing amplitudes and deduced length scales are shown in Fig. 3. As expected, the $\Delta_{m,\alpha}$ are suppressed upon increasing the magnetic field, see Fig. 3(a). As shown in Fig. 3(b,c), after a slow decrease at low B ’s, the core radii $\xi_\alpha^{(c)}$ are once again nearly constant over a wide range of field values. Most importantly however, we find at all fields that $\xi_1^{(c)} \approx \xi_2^{(c)}$, see panel (d) of Fig. 3. As B approaches the upper critical field H_{c2} , $\xi_2^{(c)}/\xi_1^{(c)} \rightarrow 1$, see Fig. 3(d). This conclusion agrees with the two-band theory of H_{c2} [25], where it has been shown that near a 2nd order phase transition at H_{c2} , the two pairing amplitudes satisfy the system of equations $-\xi^2 \Pi^2 \Delta_\alpha = \Delta_\alpha$ with the same ξ .

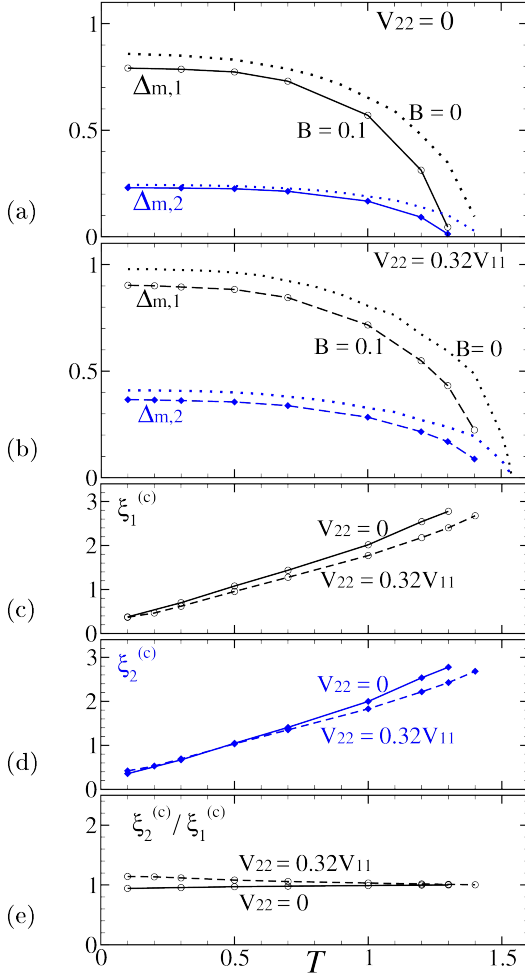


FIG. 2. (Color online) (a) Temperature dependence of maximum values $\Delta_{m,\alpha}$ of pairing amplitudes $|\Delta_\alpha(\mathbf{r})|$ at $B = 0.1$ for $V_{22} = 0$ and $V_{12} = 0.32 V_{11}$. Zero-field $|\Delta_\alpha|$ are shown by dotted lines. (b) The same as (a) for $V_{22} = 0.32 V_{11}$. (c,d) T dependences of core sizes $\xi_\alpha^{(c)}$, and (e) of $\xi_2^{(c)}/\xi_1^{(c)}$ for $B = 0.1$. Temperature T is in units of T_{c1} .

IV. DECOUPLING LIMIT $V_{12} \ll V_{11}$

Next we analyze the regime of almost decoupled band. In this limit, the two superconducting condensates are nearly independent. The vortex core radii can be different and dependent on the characteristics of the bands [7, 8].

We consider a weak inter-band coupling, $V_{12} = 0.01 V_{11}$, whereas $V_{22} = 0.85 V_{11}$. The resulting $|\Delta_\alpha(\mathbf{r})|$ are presented in Fig. 4(a). At a low field $B = 0.01$ (dashed lines), the recovery of $|\Delta_2(\mathbf{r})|$ with increasing r is indeed slow compared to $|\Delta_1(\mathbf{r})|$, and as a result we find that $\xi_2^{(c)} > \xi_1^{(c)}$. This behavior can also be seen in the r dependence of the ratio $|\Delta_2(\mathbf{r})|/|\Delta_1(\mathbf{r})|$, which is no longer constant, but decreases near the vortex core, see Fig. 4(b). For higher field, $B = 0.1$ (see the solid

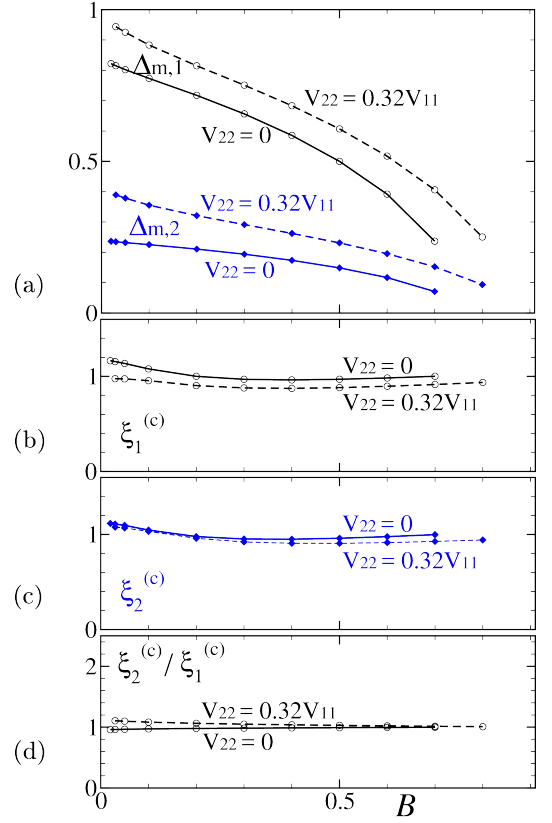


FIG. 3. (Color online) (a) Magnetic field dependence of $\Delta_{m,\alpha}$, $\alpha = 1, 2$. (b,c) B dependence of the core sizes $\xi_\alpha^{(c)}$ and (d) the ratio $\xi_2^{(c)}/\xi_1^{(c)}$. Inputs: $t = 0.5$, $V_{12} = 0.32 V_{11}$, solid lines are for $V_{22} = 0$, dashed lines for $V_{22} = 0.32 V_{11}$.

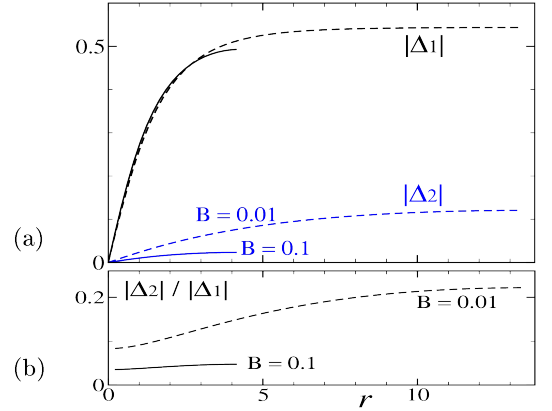


FIG. 4. (Color online) (a) $|\Delta_1(\mathbf{r})|$ and $|\Delta_2(\mathbf{r})|$ vs distance r from the vortex center to the midpoint between nearest neighbor vortices. (b) $|\Delta_2(\mathbf{r})|/|\Delta_1(\mathbf{r})|$. Input parameters are $V_{12} = 0.01 V_{11}$, $V_{22} = 0.85 V_{11}$, and $t = 0.5$; solid lines are for $B = 0.1$, dashed lines are for $B = 0.01$.

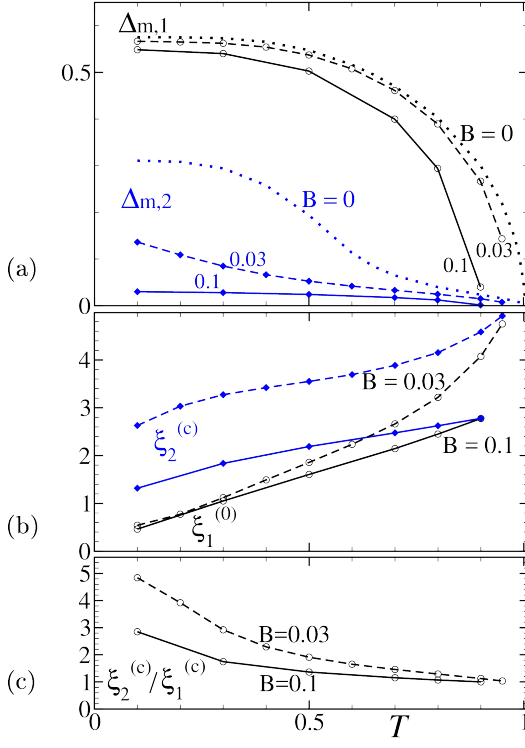


FIG. 5. (Color online) (a) Temperature dependence of $\Delta_{m,\alpha}$ at $B = 0$ (dotted lines), $B = 0.03$ (dashed lines), and $B = 0.1$ (solid lines). (b) T dependence of the vortex core radii $\xi_1^{(c)}$ and $\xi_2^{(c)}$, and (c) the ratio $\xi_2^{(c)}/\xi_1^{(c)}$. $V_{12} = 0.01V_{11}$ and $V_{22} = 0.85V_{11}$.

lines in Fig. 4), $|\Delta_1(\mathbf{r})|$ within the core region does not change substantially compared to the low-field case, whereas $|\Delta_2(\mathbf{r})|$ is suppressed strongly, as the intervortex distance is too short for the recovery of $|\Delta_2(\mathbf{r})|$. In other words, since the “effective H_{c2} ” of the second band is small due to a larger coherence length ($v_2 = 3v_1$ and Δ_2 is small), superconductivity of the second band is easily suppressed by magnetic fields. Hence, at high fields, the contribution to superconductivity of the second band is weak.

The corresponding temperature dependence of the nearly decoupled band regime is shown in Fig. 5. $\Delta_{m,1}$ has the typical T -dependence of the BCS theory. However, $\Delta_{m,2}(T)$ is different. At low T , the superconductivity of the second band is enhanced, since it is caused here by $V_{22} = 0.85V_{11}$. For $B = 0$, Δ_2 is very small at elevated temperatures. Above the intrinsic transition temperature of the decoupled second band, superconductivity of this band is only induced by the weak interband coupling V_{12} , an observation that was made already shortly after the formulation of the BCS-theory [26]. With increasing B , the enhancement of $\Delta_{m,2}$ at low T disappears and practically vanishes at $B = 0.1$. The B -dependence of the pairing amplitudes are shown in Fig. 6. $\Delta_{m,2}$ decreases rapidly at low B reflecting small effective $H_{c2,2}$

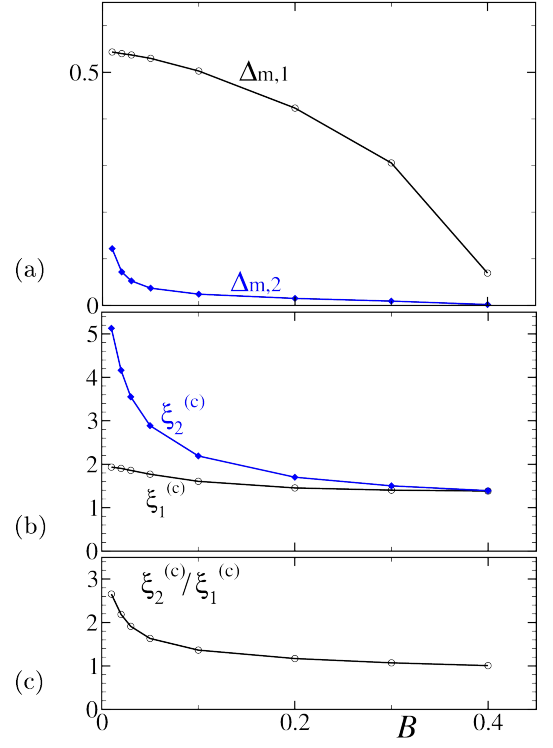


FIG. 6. (Color online) (a) The field dependence of $\Delta_{m,\alpha}$. (b) B -dependence of core radii $\xi_1^{(c)}$ and $\xi_2^{(c)}$, and (c) the ratio $\xi_2^{(c)}/\xi_1^{(c)}$. Input parameters: $t = 0.5$, $V_{12} = 0.01V_{11}$ and $V_{22} = 0.85V_{11}$.

of the second band, and remains small at higher B due to weak coupling V_{12} . In the high B range, $\xi_1^{(c)} \approx \xi_2^{(c)}$. This combination of field and temperature variation of nearly decoupled bands may serve as a tool to identify whether one is indeed in this limit.

We note that the Kramer-Pesch shrinking of $\xi_2^{(c)}$ on cooling is weak compared to that of $\xi_1^{(c)}$, see Fig. 5(b). Thus, the ratio $\xi_2^{(c)}/\xi_1^{(c)}$ increases upon lowering T . On the other hand, at higher T and for fields approaching H_{c2} , $\xi_2^{(c)}/\xi_1^{(c)} \rightarrow 1$ (again in agreement with Ref. [25]).

V. DISCUSSION

The issue of the spatial variation of the superconducting order parameter in multi-band systems is interesting and relevant, in particular because of an increasing number of physical systems that clearly display multi-band behavior in their superconducting properties. In addition to the description of the variation of the order parameter near vortex cores, the DOS distribution is related to $\Delta(\mathbf{r})$ and is measurable. Recent STM low- T data, interpreted within a phenomenological model, suggest that $\xi_1^{(c)} = \xi_2^{(c)}$ [17]. While such length-scale locking is to be expected in the immediate vicinity of the transition

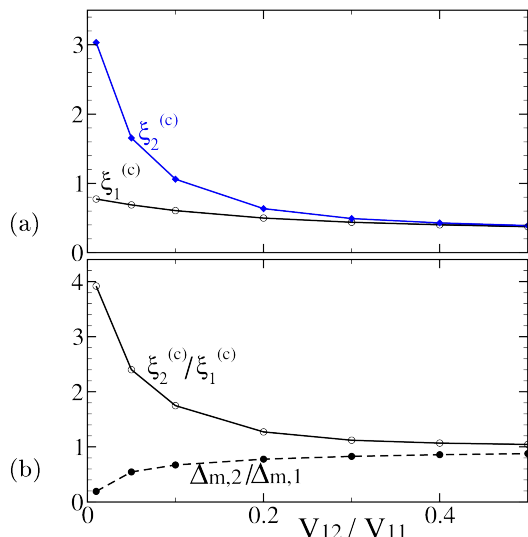


FIG. 7. (Color online) (a) $\xi_\alpha^{(c)}$ vs interband coupling V_{12}/V_{11} for $V_{22} = 0.83 V_{11}$ at $t = 0.2$ and $B = 0.03$. (b) Ratios $\xi_2^{(c)}/\xi_1^{(c)}$ and $\Delta_{m,2}/\Delta_{m,1}$ vs V_{12}/V_{11} for the same parameters as (a).

temperature, it is not obvious away from T_c . Thus, a microscopic analysis of this open question is timely and relevant. It shows that, within the accuracy of our numerical routines, $\xi_1^{(c)} \approx \xi_2^{(c)}$ if the inter-band coupling is of the same order as intra-band ones. This conclusion turns out to be valid at all temperatures and fields. In agreement with other microscopic calculations [7, 8], we find this rule is violated for a very weak inter-band coupling when the system is close to the limit of nearly decoupled condensates. The peculiar field and temperature dependence of such nearly decoupled bands can easily be used to test, for a given material, whether the coupling between bands is weak or only moderate.

To make this statement more quantitative, we show in Fig. 7 the ratio $\xi_2^{(c)}/\xi_1^{(c)}$ as a function of the interband coupling V_{12}/V_{11} at fixed $t = T/T_{c1} = 0.2$ and $B = 0.03$. One sees that this ratio exceeds the value of 2 only when roughly $V_{12}/V_{11} < 0.1$. As discussed above, MgB_2 can be very well described by $V_{12}/V_{11} \approx 0.2$ (see Refs. [9, 11–14]). Thus, we conclude that this systems is not in the limit where two distinct characteristic length scales emerge.

In conclusion, by solving the quasi-classical Eilenberger equations, we analyzed the spatial variation of the pairing amplitudes within the vortex lattice of a two band superconductor over a wide range of temperatures and magnetic fields. Near the superconducting transition temperature $T_c(B)$, it is established [1–3, 25] that the emergence of one order parameter naturally implies that the spatial variation of this order parameter is governed by a single length scale. Away from T_c it is however natural to expect that for a sufficiently weak coupling between the bands, distinct characteristic length scales

for the respective pairing amplitudes emerge. However, what precisely is meant by *sufficiently weak* has not been investigated thus far. Here we showed that such decoupling of the length scales occurs for values of the interband pairing interaction V_{12} that is less than one order of magnitude of the largest intraband coupling. For larger values of the interband coupling a common temperature variation of the length $\xi_1^{(c)}$ and $\xi_2^{(c)}$ of the pairing amplitudes sets in. What is most surprising about our results is that these two length scales not only follow a common T -dependence, they are essentially identical in their magnitude $\xi_1^{(c)} \approx \xi_2^{(c)}$. In other words, we observe a robust length scale locking of moderately coupled multiband superconductors. Whatever difference might there be in the values of the length scales of the uncoupled system, our analysis shows that this difference is most likely to disappear everywhere below $H_{c2}(T)$.

In this work we only considered the situation of a clean two-band situation. Usually, the impurity scattering is expected to cause an isotropization of superconducting characteristics. Hence, we do not expect scattering to amplify differences of the length scales ξ_α . Still, as discussed in Ref. [16], inter-band scattering can cause the superconductivity to become gapless with two bands acquiring substantially different DOSs in superconducting state. The question of how this difference affects ξ_α remains to be answered.

ACKNOWLEDGEMENTS

We thank Lev Boulaevskii for illuminating comments. Work of V.K. was supported by the U.S. Department of Energy, Office of Science, Basic Energy Sciences, Materials Sciences and Engineering Division. The Ames Laboratory is operated for the U.S. DOE by Iowa State University under Contract No. DE-AC02-07CH11358.

Appendix A: Numerical method

We briefly summarize the numerical approach to solve the coupled Eilenberger equations Eqs. (1). For the numerical analysis, it is more convenient to employ instead of the function f and g the functions a and b defined via

$$f = \frac{2a}{1+ab}, \quad f^+ = \frac{2b}{1+ab}, \quad g = \frac{1-ab}{1+ab} \quad (\text{A1})$$

and transform the system (1)-(2) to Ricatti differential equations,

$$\mathbf{v} \cdot \nabla a = (\Delta - \Delta^* a^2) - (\omega + i\mathbf{v} \cdot \mathbf{A})a, \quad (\text{A2})$$

$$-\mathbf{v} \cdot \nabla b = (\Delta^* - \Delta b^2) - (\omega + i\mathbf{v} \cdot \mathbf{A})b, \quad (\text{A3})$$

for each band α [27]. Unlike the original Eqs. (1), the equations for a and b are decoupled. The Ricatti equations are then solved by numerical integration along trajectories parallel to the vector \mathbf{v} [28]. Choosing length

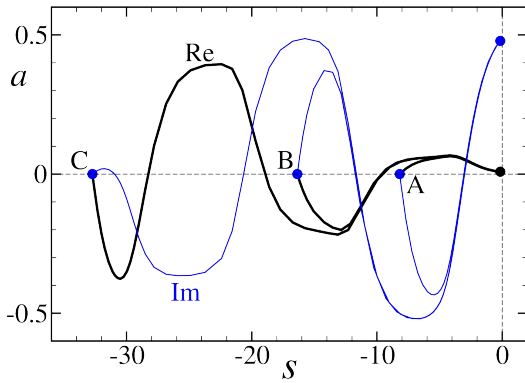


FIG. 8. (Color online) Solving the first-order ordinary differential Eq. (A2) along the trajectory $\mathbf{r}' = \mathbf{r} + s\hat{\mathbf{v}}_\alpha$ for a at $s = 0$. Real and imaginary part of a are shown for start positions $s_0 = -8.2$ (A), -16.4 (B) and -32.7 (C). It is seen, that a converges to the same solution at $s = 0$. Input parameters are $\phi = 1.25^\circ$ for \mathbf{k} , $\alpha = 1$, $\omega = \pi T$ and $V_{22} = 0$ in the case of Fig. 1. \mathbf{r} is near the midpoint $(-a_0/2, 0)$ between nearest neighbor vortices.

$|s_0|$ of these trajectories in Fig. 8, we confirm that the solution does not change when this length is increased. We iterate the set of equations until self-consistent results are obtained.

-
- [1] B. T. Geilikman, R. O. Zaitsev, and V. Z. Kresin, Sov. Phys. Solid State **9**, 642 (1967).
 - [2] J. Geyer, R. M. Fernandes, V. G. Kogan, and J. Schmalian, Phys. Rev. B **82**, 104521 (2010).
 - [3] V. G. Kogan and J. Schmalian, Phys. Rev. B **83**, 054515 (2011).
 - [4] E. Babaev and M. Speight, Phys. Rev. B **72**, 180502 (2005).
 - [5] E. Babaev, J. Calström, M. Silaev, and J.M. Speight, arXiv:1608.02211.
 - [6] V. Moshchalkov, M. Menghini, T. Nishio, Q. H. Chen, A.V. Silhanek, V. H. Dao, L. F. Chibotaru, N. D. Zhigadlo, and J. Karpinski, Phys. Rev. Lett. **102**, 117001 (2009).
 - [7] M. Silaev and E. Babaev, Phys. Rev. B **84**, 094515 (2011).
 - [8] L. Komendova, Yajiang Chen, A. A. Shanenko, M.V. Milosevic, and F. M. Peeters, Phys. Rev. Lett. **108**, 207002 (2012).
 - [9] I. I. Mazin and V. P. Antropov, Physica C **385**, 49 (2003).
 - [10] G. Blumberg, A. Mialitsin, B. S. Dennis, M. V. Klein, N. D. Zhigadlo, and J. Karpinski, Phys. Rev. Lett. **99**, 227002 (2007).
 - [11] A.Y. Liu, I. I. Mazin and J. Kortus, Phys. Rev. Lett., **87**, 087005 (2001).
 - [12] A. A. Golubov, J. Kortus, O. V. Dolgov, O. Jepsen, Y. Kong, O. K. Andersen, B. J. Gibson, K. Ahn and R. K. Kremer, J. Phys.: Condens. Matter **14**, 1353 (2002).
 - [13] H. J. Choi, D. Roundy, H. Sun, M. L. Cohen, and S. G. Louie, Phys. Rev. B **66**, 020513 (2002).
 - [14] H. J. Choi, D. Roundy, H. Sun, M. L. Cohen, and S. G. Louie, Nature **418**, 758 (2002).
 - [15] I. I. Mazin and J. Schmalian, Phys. C: Supercond. **469**, 614 (1995).
 - [16] V. G. Kogan and R. Prozorov, Phys. Rev. B **93**, 224515 (2016).
 - [17] A. Fente, E. Herrera, I. Guillamon, H. Suderow, S. Mañas-Valero, M. Galbiati, E. Coronado and V. G. Kogan, Phys. Rev. B **94**, 014517 (2016).
 - [18] A. Fente, W. R. Meier, T. Kong, V.G. Kogan, S. L. Bud'ko, P. C. Canfield, I. Guillamon, H. Suderow, arXiv:1608.00605.
 - [19] M. Ichioka, K. Machida, N. Nakai, and P. Miranović, Phys. Rev. B **70**, 144508 (2004).
 - [20] G. Eilenberger, Z. Phys. **214**, 195 (1968).
 - [21] M. Ichioka, N. Hayashi, and K. Machida, Phys. Rev. B **55**, 6565 (1997).
 - [22] L. Kramer and W. Pesch, Z. Phys. **269**, 59 (1974).
 - [23] M. Ichioka, N. Hayashi, N. Enomoto, and K. Machida Phys. Rev. B **53**, 15316 (1996).
 - [24] A. Gumann, S. Graser, T. Dahm, and N. Schopohl, Phys. Rev. B **73**, 104506 (2006).
 - [25] V. G. Kogan and R. Prozorov, Rep. Prog. Phys. **75**, 114502 (2012).
 - [26] H. Suhl, B. T. Matthias, and L. R. Walker, Phys. Rev. Lett. **3**, 552 (1959).
 - [27] N. Schopohl and K. Maki, Phys. Rev. B **52**, 490 (1995).
 - [28] P. Miranović, M. Ichioka, and K. Machida, Phys. Rev. B **70**, 104510 (2004).